

# Relationship of brain and skull in pre- and postoperative sagittal synostosis

Kristina Aldridge,<sup>1</sup> Alex A. Kane,<sup>2</sup> Jeffrey L. Marsh,<sup>3</sup> Peng Yan,<sup>1</sup> Daniel Govier<sup>2</sup> and Joan T. Richtsmeier<sup>1,4</sup>

<sup>1</sup>Department of Anthropology, The Pennsylvania State University, USA

<sup>2</sup>Cleft Palate and Craniofacial Deformities Institute, St. Louis Children's Hospital, Section of Pediatric Plastic Surgery, Washington University School of Medicine, St Louis, Missouri, USA

<sup>3</sup>Cleft Lip/Palate and Craniofacial Deformities Center, Kids Plastic Surgery, St John's Mercy Medical Center, St Louis, Missouri, USA

<sup>4</sup>Center for Craniofacial Development and Disorders, The Johns Hopkins Hospital, Baltimore, Maryland, USA

---

## Abstract

Models of vertebrate skull evolution stress the coordinated developmental relationship between the skull and the brain that it houses. This study investigates the relationship between altered skull morphology and brain morphology in premature fusion of the cranial sagittal suture (isolated sagittal synostosis; ISS), a condition associated with dysmorphology of both neurocranium and brain. Although the skull displays a more normal shape following reconstructive cranial vault surgery, effects of this surgery on the brain have not been investigated. Landmark coordinate data were collected from three-dimensional magnetic resonance imaging reconstructions of the brain in a sample of ISS patients and an age-matched unaffected cohort. These data were analysed using Euclidean distance matrix analysis (EDMA). Results show that the brain in ISS is dysmorphic preoperatively, displaying a posteriorly directed neural expansion that does not 'worsen' with growth. Postoperatively, the brain in ISS displays a more globular shape overall as compared with the preoperative morphology, but differs from normal in its subcortical morphology. These results show that the ISS brain is altered following neurocranial surgery, but does not more closely approximate that of unaffected individuals. This suggests that although the brain is affected by manipulation of the skull, it retains a growth pattern that is, at least in part, independent of the skull.

**Key words** craniosynostosis; shape; skull; suture.

## Introduction

Craniosynostosis has been defined as the premature fusion of one or more of the cranial sutures and occurs in roughly 1 in 2000 live births, with isolated sagittal synostosis (ISS) accounting for 57% of isolated synostosis cases (Cohen & MacLean, 2000). The diagnostic phenotype in ISS is characteristic dysmorphology of the craniofacial complex. This dysmorphology includes an antero-posteriorly expanded neurocranium (scaphocephaly), increased head circumference, bony ridging over the sagittal suture, biparietal and bitemporal narrowing, and exaggerated frontal and occipital prominences

(Marsh & Vannier, 1986; Kaiser, 1988; Richtsmeier et al. 1991). Diagnosis is confirmed by radiographic evidence of a non-patent sagittal suture between the paired parietal bones (Fig. 1). Although craniosynostosis was first diagnosed on the basis of the skeletal phenotype (Virchow, 1851), abnormal growth of the brain was proposed by some as the primary factor leading to the overall phenotype observed in craniosynostosis (e.g. Moss & Young, 1960; Moss, 1962). We have previously described the dysmorphic brain phenotype in ISS prior to corrective cranial vault surgery (Aldridge et al. 2002).

Corrective calvarial surgery was originally proposed to relieve suspected increased intracranial pressure (ICP) in cases of craniosynostosis, although the existence of ICP has been questioned (Carmel et al. 1981; Cohen & Persing, 1998; Mouradian, 1998). More recently, the emphasis for reconstructive surgery has been placed on the achievement and maintenance of a normative skull shape (Barritt et al. 1981; Marsh, 2000; Renier et al.

---

### Correspondence

Dr Kristina Aldridge, Department of Anthropology, Pennsylvania State University, 409 Carpenter Building, University Park, PA 16802, USA. T: +1 814 865 2066; F: +1 814 863 1474; E: kja3@psu.edu

Accepted for publication 26 January 2005

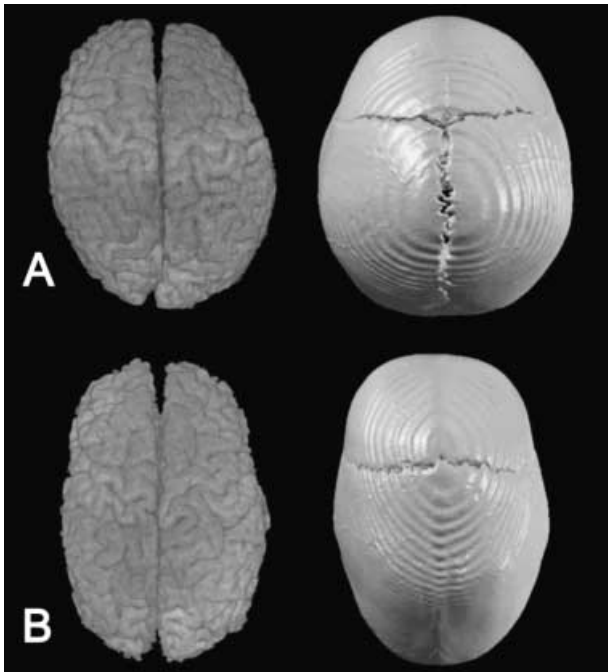


**Fig. 1** Superior view of CT and MRI reconstructions of the skull and the brain of a child unaffected by craniosynostosis (A) and a child affected by isolated sagittal synostosis (B).

2000). Contemporary treatment protocols recommend reconstructive surgery during the first year of life to correct and prevent possible further damage to the brain. Equally important is the prevention of psychological trauma that may occur in children with craniofacial dysmorphology. Patients are carefully monitored during childhood to document central nervous system morbidity and/or recurrent dysmorphology (Barritt et al. 1981; Renier et al. 2000).

Previous studies have quantified and described changes in skull morphology following corrective surgery, suggesting that the skull is returned to a more 'normal' morphology (Kreiborg & Pruzansky, 1981; Kaiser, 1988; Marsh et al. 1991; Posnick et al. 1993; DeLeon et al. 2001; Perlyn et al. 2001). Although the primary motivation expressed for reconstructive surgery in ISS is release of the fused suture to free a constrained brain, the morphology of the brain has not been studied to the extent of either skeletal or dural morphology. Although the brain of craniosynostosis individuals has been described as 'normal' in the sense that all of the component structures are present, it clearly is abnormal in shape (Marsh et al. 1997; Cooper et al. 1999). We do not know the relative roles of abnormal growth of the skull and of the brain in the production of the ISS phenotype.

Owing to previous and current standards of care we may never know the incidence of brain damage in untreated ISS. An available step that is vital to the delineation of these relationships is to determine the effect, if any, of corrective cranial vault surgery on the brain.

Previous studies of brain morphology in craniosynostosis have reported primarily qualitative observations, or have measured relative volumes or sizes of the entire brain or cranial cavities, with varying results. Gault et al. (1992) found that changes in skull shape were mirrored by similar changes in the underlying brain, but found intracranial volume to be within or above normal limits in children affected by various forms of craniosynostosis (Gault et al. 1990, 1992; Fok et al. 1992). Other studies, however, have found intracranial volume to be reduced in ISS patient samples (Dufresne et al. 1987; Posnick et al. 1992, 1995).

It is difficult to compare the results of these studies owing to the confusion created by including more than one type of synostosis in a study sample (Singhal et al. 1997). Fusion of a particular suture is produced by, and results in, a unique set of events culminating in specific morphologies. Distinct morphologies of the neurocranium and cranial base are known for each type of craniosynostosis but less is known of changes that occur in the brain. Qualitative assessment and measures of overall brain volume provide little information regarding specific effects of craniosynostosis on neural tissue. The heterogeneous nature of the brain requires a more localized, quantitative investigation of the neural phenotype in craniosynostosis. An understanding of the etiology of craniosynostosis in all of its forms requires thorough investigation of the skeletal and neural phenotype in each diagnostic category individually.

This study investigates brain morphology in pre- and postoperative ISS patients. Patterns of brain morphology in children affected by ISS are compared with those of morphologically normal children to supplement the information presented by Aldridge et al. (2002). Patterns of morphology are also compared between ISS and age-matched unaffected individuals 1 year following neurocranial surgery on the synostosis group to determine how surgical alteration of the skull affects underlying brain morphology.

## Materials and methods

The study sample includes whole brain magnetic resonance images (MRIs) of 43 human infants from St. Louis

**Table 1** Diagnosis, age and sex distribution of the study sample of 32 ISS patients and 11 unaffected individuals. Nine of the 32 ISS patients had both pre- and postoperative MRIs; one ISS patient had only a postoperative scan

Diagnosis	Age (weeks)	N
Samples at Age A		
Preoperative sagittal synostosis	10–43	28 (23M, 5F)
Unaffected	14–50	6 (4M, 2F)
Samples at Age B		
Preoperative sagittal synostosis	72–105	3 (3F)
Postoperative sagittal synostosis	68–116	10 (8M, 2F)
Unaffected	72–107	5 (1M, 4F)

Children's Hospital ( $n = 52$  MRIs; Table 1). This number includes 32 ISS patients and 11 age-matched unaffected individuals. The entire sample was divided into two age groups, Age A and Age B. Our sample includes children affected with ISS imaged just prior to surgery at Age A and at Age B, 1 year after subtotal calvarial vault remodelling surgery at Age B, and a sample of age-matched children at Age A and Age B unaffected by craniosynostosis (see Fig. 3). Nine of the 32 ISS patients had both pre- and postoperative images, while one ISS patient had only a postoperative scan.

Only one of the children with ISS had a positive family history of craniosynostosis. No differences were

observed in results of analyses performed both including and excluding this individual, so we include this individual in the analyses reported here. Children unaffected by craniosynostosis were imaged due to suspected medical conditions (i.e. supposed concussion, unexplained seizures), but were subsequently determined to display no abnormalities.

Three-dimensional landmark coordinate data were collected from MRIs of the brain of each individual. Thirty-two landmarks were defined on cortical and subcortical structures (Table 2 and Fig. 2). All non-neural tissue was stripped from each image slice following a semi-automated procedure described by Aylward et al. (1997) and Buchanan et al. (1998). A three-dimensional (3D) reconstruction of the remaining brain tissue was produced from the stripped slice data, which is manipulated in virtual space and viewed from any direction. The 3D coordinate location of each landmark was collected for each individual using MEASURE software (Barta et al. 1997), written for a PC platform. This software allows visualization of MRI data and placement of landmarks in any three orthogonal planes and in a 3D reconstruction.

Anatomical landmarks are biologically meaningful specific loci that can be repeatedly located with a high degree of accuracy and precision (Richtsmeier et al. 1995; Valeri et al. 1998). Measurement error was evaluated following methods presented previously (Aldridge et al. 2000) and minimized statistically by digitizing

**Table 2** Definitions of landmarks collected from MRIs. Landmarks illustrated in Fig. 2 are keyed to the landmark number

Landmark no.	Landmark definition
1, 2	Frontal pole (left, right)
3, 4	Posterior termination of the superior frontal sulcus (left, right)
5, 6	Posterior termination of the inferior frontal sulcus (left, right)
7, 8	Inferolateral termination of the central sulcus (left, right)
9, 10	Posterior termination of the Sylvian fissure (left, right)
11, 12	Occipital pole (left, right)
13, 14	Anterior horn of the lateral ventricle (left, right)
15, 16	Centroid of the head of the caudate nucleus (left, right)
17, 18	Centroid of the thalamus (left, right)
19, 20	Centroid of the amygdala (left, right)
21, 22	Posterior horn of the lateral ventricle (left, right)
23	Midline of the most superior aspect of the pons
24	Midline of the most inferior aspect of the pons
25	Midline of the genu of the corpus callosum
26	Midline of the posterior commissure
27, 28	Centroid of the superior colliculus (left, right)
29, 30	Centroid of the inferior colliculus (left, right)
31	Junction of the cerebral aqueduct and the 4th ventricle
32	Posterior-most aspect of the 4th ventricle

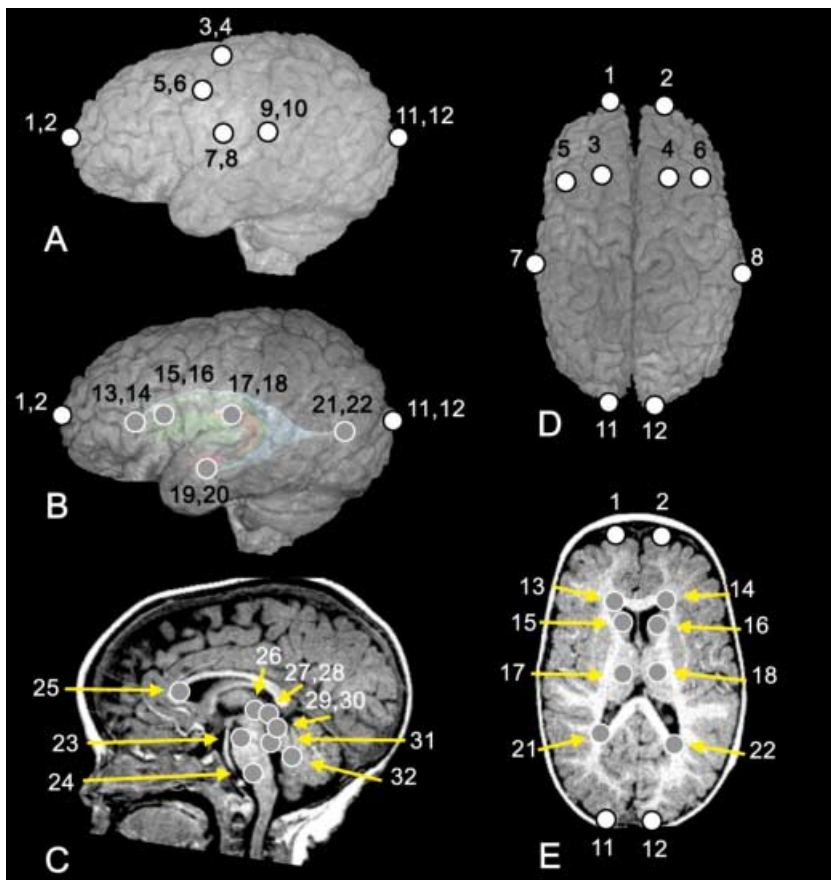


**Fig. 2** Landmarks collected for analysis, illustrated on an MRI of a patient with ISS. (A) Left lateral view of the 3D surface illustrating cortical surface landmarks. (B) Left lateral view of the 3D surface with a model of subcortical structures ghosted beneath illustrating subcortical landmarks with respect to surface topography. (C) Midsagittal slice illustrating near midline subcortical landmarks. (D) Superior view of the 3D surface illustrating cortical surface landmarks. (E) Transverse slice illustrating subcortical landmarks. White dots represent landmarks located on the cortical surface, whereas grey dots represent landmarks located on subcortical structures. Numbers refer to landmark definitions given in Table 2.

each specimen twice, checking for overt or gross error, and using the average of two trials for analysis to reduce intraobserver error.

The landmark coordinate data recorded in MEASURE were analysed using Euclidean Distance Matrix Analysis (EDMA; Lele & Richtsmeier, 2001). This is a linear distance-based morphometric method that does not rely on registration or any particular smoothness criteria (Lele, 1993; Lele & Richtsmeier, 2001; Lele & McCulloch, 2002). Briefly, for each individual in the study sample, 3D landmark coordinates of biological points are converted into a matrix of linear distances between all unique landmark pairs. To compare brain shapes, corresponding linear distances are compared across individuals, or across samples, as the ratio of similar linear distances. If a given ratio is equal to 1, the samples being compared do not differ with respect to the specific linear distance. If a ratio differs from 1, the samples differ for that linear distance.

Using EDMA, the 3D morphology of samples of biological forms can be compared statistically through null hypothesis testing of discrete linear distances. The null

hypothesis tested is that the samples being compared do not differ with respect to a given linear distance, i.e. the ratio for that particular linear distance is equal to 1. Confidence intervals for statistical evaluation of similarity of individual linear distances are reported using an alpha level of 0.10. Our criteria for considering a specific linear distance important to phenotypic difference between samples includes (1) reaching statistical significance, and (2) differing by at least 10% between samples. Discrete linear distances determined to be significantly different by confidence interval testing and which differed by 10% or more are illustrated (Figs 4–7). Distances that were found to be statistically different between samples but that did not meet the criterion of a 10% increase or decrease in length are not illustrated, but are available from the authors upon request.

Four sets of comparisons were performed and are illustrated in Fig. 3. (1) Preoperative ISS children were compared with age-matched unaffected children at Age A to define the difference in patterns of brain morphology between affected and unaffected individuals at Age A. (2) Preoperative ISS children were compared

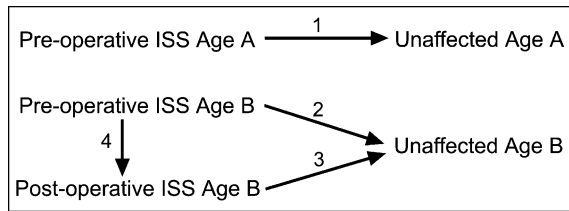


**Fig. 3** Illustration of the four sets of comparisons performed in this study.

with age-matched controls at Age B to define the differences in patterns of brain morphology between affected and unaffected individuals at Age B. (3) Post-operative ISS children at Age B were compared with age-matched unaffected children to define significant patterns of differences in brain morphology between affected and unaffected individuals following cranial vault surgery with the additional factor of surgery on the cranial vault. (4) Preoperative ISS children at Age B were compared with age-matched postoperative children to specify the effects of alterations in the cranial vault on patterns of morphology in the underlying brain.

## Results

Results of our analyses are illustrated for each set of comparisons (Figs 4–7).

### Preoperative ISS at Age A vs. unaffected at Age A

Results of the comparisons of younger preoperative ISS patients and age-matched unaffected individuals are illustrated on the brain of a preoperative ISS patient in Fig. 4. Red and yellow lines indicate linear distances that are statistically greater in the ISS patient sample, and the single white line indicates a linear distance that is significantly smaller in the ISS patient sample.

The overall pattern of difference revealed by statistical comparison of these two groups indicates a brain that is longer anteroposteriorly in ISS than in the unaffected sample. This anteroposterior lengthening is accomplished through the expansion of localized regions in an anteroposterior (AP) direction, with little difference either mediolaterally or superoinferiorly. Many of the differences can be localized to the occipital poles, with the relationships of the occipital poles to many structures located anterior to them greater in the younger preoperative sample as compared with the younger unaffected sample (Fig. 4A,B). This indicates a disproportionate posterior displacement of the occipital region relative to the rest of the brain in the average ISS brain. There are also anteroposterior expansions between some of the centrally located structures, including those between the anterior lateral ventricles and the thalami, and between the posterior lateral ventricles and the thalami (Fig. 4B,C).

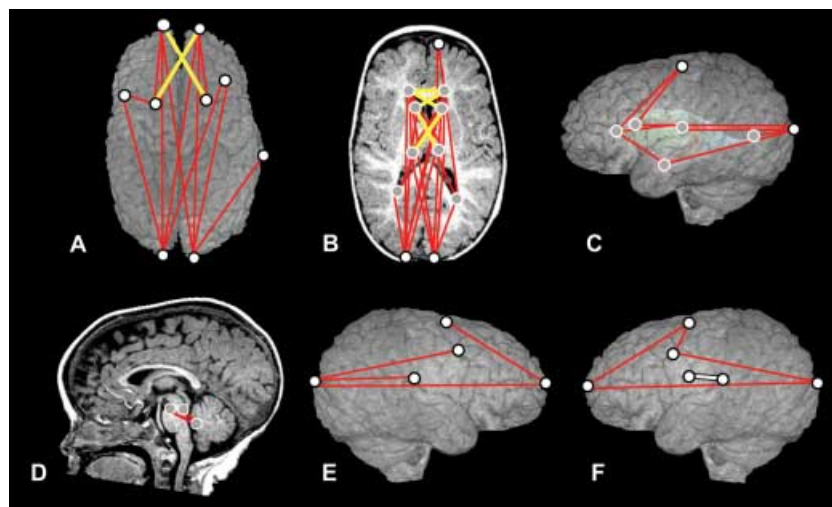


**Fig. 4** Comparisons of preoperative ISS vs. unaffected at Age A, shown on MRI reconstructions of a preoperative ISS patient. The top row represents a superior view of the cortical surface (A), a transverse slice displaying subcortical structures (B) and the left lateral view of the 3D surface with a model of subcortical structures ghosted beneath (C). The bottom row represents a midsagittal slice (D), a right lateral view of the 3D reconstruction of the cortical surface (E) and a left lateral view of the 3D reconstruction of the cortical surface (F). White dots represent landmarks located on the cortical surface, and grey dots represent landmarks located on subcortical structures. Red and yellow lines indicate linear distances that are significantly greater in the ISS sample, and the white line (F) indicates the single linear distance that is significantly smaller in the ISS sample.

Although the majority of the difference is observed in anteroposterior changes, there are a limited number of focal areas where there is also oblique mediolateral widening. The frontal region displays a mediolateral widening between the left and right anterior lateral ventricles and between the ventricles and contralateral caudate nuclei (Fig. 4B, yellow lines). This is also evident in the cortical surface, in the relationship between the frontal poles and the contralateral superior frontal sulci (Fig. 4A, yellow lines). Furthermore, oblique mediolateral distances between the caudate nuclei and contralateral thalami are increased in brains of children with ISS (Fig. 4B, yellow lines).

The hindbrain also differs between the younger preoperative and the younger unaffected samples (Fig. 4D). The distances between the superior and posterior aspects of the 4th ventricle, and between the superior aspect of the pons and posterior 4th ventricle are greater in the younger preoperative sample. These differences indicate a posteroinferior shift in the younger preoperative hindbrain region relative to what is seen in the normal condition.

The single linear distance that is significantly smaller in the younger preoperative sample as compared with the younger unaffected sample is located between the left Sylvian fissure and the left central sulcus (Fig. 4F), indicating a localized constriction of the cortex in that

region. No other linear distances were significantly smaller by 10% or more in the younger preoperative sample, although there were four significantly different linear distances that differed by 6–7%.

These results considered together indicate a greatly increased anteroposterior dimension in the younger preoperative ISS sample as compared with the younger unaffected sample, with concomitant oblique mediolateral widening in specific locations of the frontal region and the subcortex. However, there is no mediolateral widening evident in cortical morphology outside of the frontal region. Although the majority of differences between ISS and normal brains at Age A can be localized to landmarks located on the occipital poles, it is difficult to determine the source of these differences as they could result from posterior displacement of the occipital poles, or from an anterior displacement of the remainder of the cortex and the subcortical structures relative to the occipital poles. These possibilities are considered in the Discussion.

#### Preoperative ISS at Age B vs. unaffected at Age B

Results of the comparison of the brains of older preoperative ISS individuals and age-matched unaffected individuals at Age B are illustrated on the brain of a preoperative ISS patient of Age B in Fig. 5. Red lines

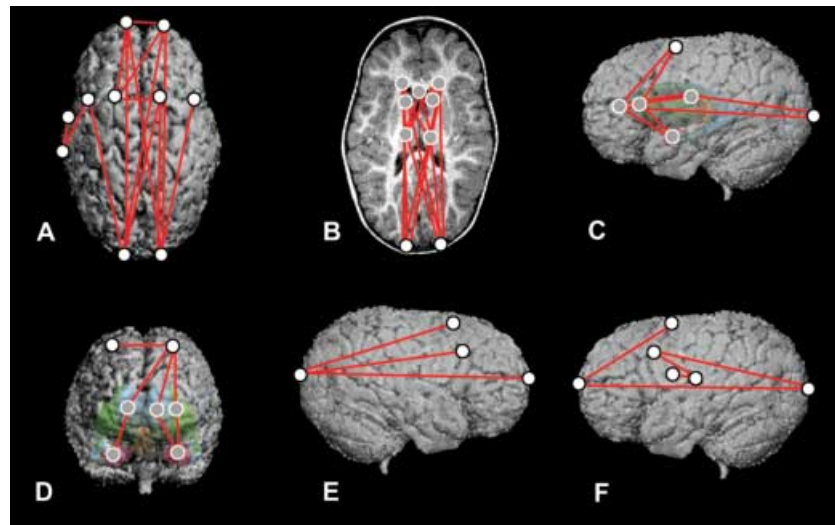


**Fig. 5** Comparisons of preoperative ISS vs. unaffected at Age B, shown on MRI reconstructions of a preoperative ISS patient. The top row represents a superior view of the cortical surface (A), a transverse slice displaying subcortical structures (B) and the left lateral view of the 3D surface with a model of subcortical structures ghosted beneath (C). The bottom row represents a midsagittal slice (D), a right lateral view of the 3D reconstruction of the cortical surface (E) and a left lateral view of the 3D reconstruction of the cortical surface (F). White dots represent landmarks located on the cortical surface, and grey dots represent landmarks located on subcortical structures. Red lines indicate linear distances that are significantly greater in the ISS sample; there are no linear distances that are significantly smaller in the ISS sample.

indicate linear distances that are significantly increased in the ISS patient sample.

Distances that are observed to be relatively larger in the ISS patient sample are again primarily oriented anteroposteriorly. This AP expansion is observed across the cortical surface (Fig. 5A,E,F), absent subcortically in the frontal region, but prevalent in the parietal and occipital subcortical regions (Fig. 5B). Differences in measures along the AP axis extend from the frontal poles and the occipital poles to one another and sites in between, including the frontal sulci (Fig. 5A,E,F). In addition, distances between the left Sylvian fissure and the left central sulcus and the left inferior frontal sulcus are elongated (Fig. 5A,F), indicating an anteroposterior expansion of this cortical region.

The distances between the anterior lateral ventricles and caudate nuclei to the ipsilateral superior frontal sulci and amygdalae are larger in the preoperative group at Age B, indicating increased superoinferior height in the frontal region (Fig. 5C,D).

There are also expansions observed along the medio-lateral axis in the frontal cortex, with the distances between the frontal poles and between the superior frontal sulci in the preoperative sample exceeding those of the unaffected group at this age (Fig. 5A). Concomitant changes in the underlying subcortex are not observed.

The sample size for the ISS group at Age B is relatively small because reconstructive surgery is usually performed during the first year of life. Consequently, these results can only be considered to be preliminary. However, given the rarity of individuals with ISS in this age group, we feel it important to include the available information. Future research including additional individuals will determine whether these results are representative of untreated ISS at this age.

#### Postoperative ISS at Age B vs. unaffected at Age B

Results of the comparison of brain morphology in postoperative ISS and age-matched unaffected individuals at Age B are illustrated on the brain of a postoperative ISS patient in Fig. 6. Red lines indicate linear distances that are significantly increased in the ISS patient sample, whereas white lines indicate linear distances that are significantly reduced in the ISS patient sample.

In sharp contrast to the comparisons of preoperative morphology with the unaffected groups, the increased anteroposterior dimensions observed in the preoperative ISS samples are not observed in the postoperative ISS group. Additionally, the preoperative comparisons did not display linear distances that were reduced in ISS as compared with normal, whereas the brain in

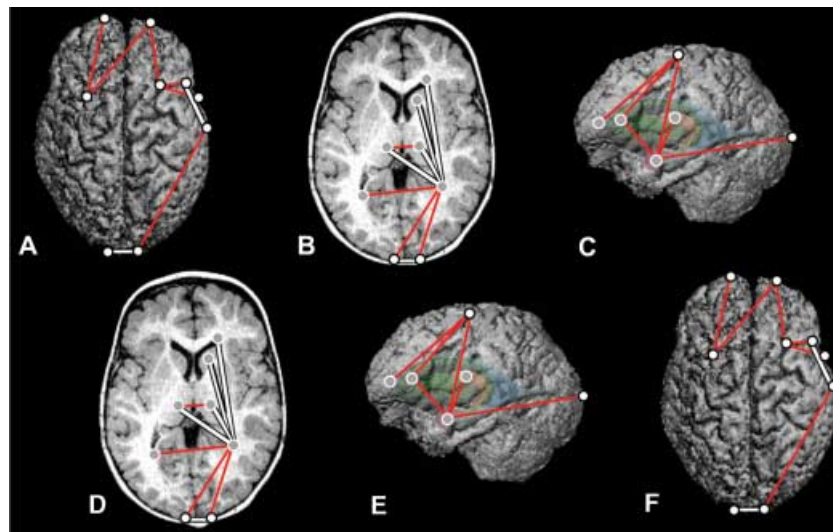


**Fig. 6** Comparisons of postoperative an ISS sample and unaffected sample at Age B, shown on MRI reconstructions of a postoperative ISS patient. The top row represents a superior view of the cortical surface (A), a transverse slice displaying subcortical structures (B) and the left lateral view of the 3D surface with a model of subcortical structures ghosted beneath (C). The bottom row represents a midsagittal slice (D), a right lateral view of the 3D reconstruction of the cortical surface (E) and a left lateral view of the 3D reconstruction of the cortical surface (F). White dots represent landmarks located on the cortical surface, and grey dots represent landmarks located on subcortical structures. Red lines indicate linear distances that are significantly greater in the postoperative ISS sample, and white lines indicate linear distances that are significantly smaller.

postoperative ISS displays many distances that are reduced (Fig. 6, white lines).

The differences between the postoperative ISS and the age-matched unaffected samples are highly localized. Distances that are longer anteroposteriorly in the postoperative ISS group are limited to the frontal and occipital regions. The distances between the frontal poles and superior frontal sulci are increased in the postoperative ISS sample (Fig. 6A,E,F), as are the distances between the occipital poles and the posterior horn of the right lateral ventricle.

In contrast, the distances between subcortical forebrain structures display significantly reduced distances along the anteroposterior axis in the postoperative ISS sample. These distances converge to the right posterior lateral ventricle from the right anterior lateral ventricle and thalamus, and both caudate nuclei (Fig. 6B). This pattern is not seen on the left side. This indicates significant anterior displacement of the posterior horn of the right lateral ventricle in postoperative ISS.

The linear dimensions between the superior frontal sulci and the anterior lateral ventricles, caudate nuclei, amygdalae (Fig. 6C) and the right central sulcus (Fig. 6A,E) are all greater in the postoperative ISS sample compared with the older unaffected sample. The distances between each amygdala and their ipsilateral caudate nuclei and thalami are greater in the postoperative ISS

sample as well (Fig. 6C,D). These results together indicate that brains of the postoperative ISS sample are larger along the superoinferior axis than those of the unaffected sample at Age B.

In contrast to the two previous comparisons, brains from the postoperative ISS sample display regions that exceed mediolateral dimensions of the unaffected sample. Neural breadths that are larger in the postoperative ISS sample include those measured between right and left amygdalae (Fig. 6D), between the right and left posterior lateral ventricles, and between the right and left thalami (Fig. 6B).

### Postoperative ISS at Age B vs. preoperative ISS at Age B

Results of the comparison of brain morphology in postoperative ISS patients and age-matched preoperative ISS patients are illustrated on the brain of a preoperative ISS patient of Age B in Fig. 7. Linear distances that are greater in the postoperative group are illustrated in red; linear distances that are reduced in the postoperative ISS sample are illustrated in white.

Distances that are greater in the postoperative group as compared with the preoperative sample at Age B are generally oriented mediolaterally and superoinferiorly. These distances are also located primarily in

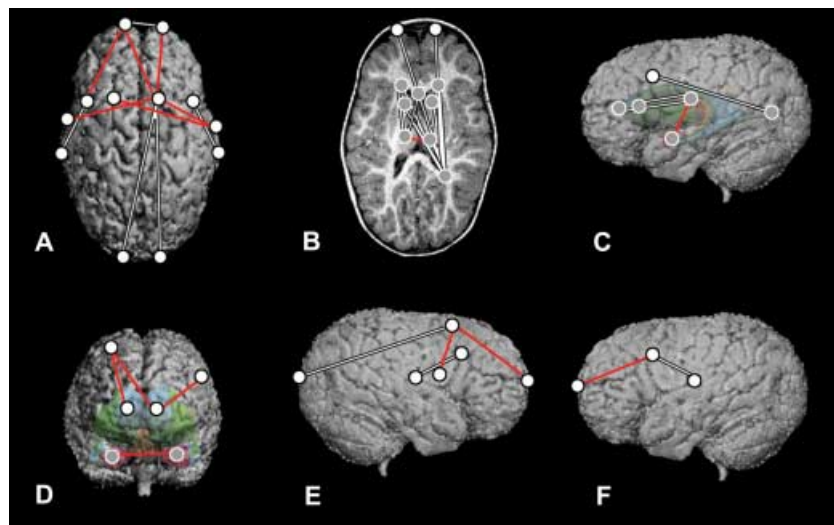


**Fig. 7** Comparisons of postoperative ISS and preoperative ISS samples at Age B, shown on a preoperative ISS patient. The top row represents a superior view of the cortical surface (A), a transverse slice displaying subcortical structures (B) and the left lateral view of the 3D surface with a model of subcortical structures ghosted beneath (C). The bottom row represents a midsagittal slice (D), a right lateral view of the 3D reconstruction of the cortical surface (E) and a left lateral view of the 3D reconstruction of the cortical surface (F). White dots represent landmarks located on the cortical surface, and grey dots represent landmarks located on subcortical structures. Red lines indicate linear distances that are significantly greater in the postoperative sample; white lines indicate those that are significantly smaller in the postoperative sample.

anterior structures. Subcortically, the distances between contralateral amygdalae (Fig. 7D), between contralateral thalami (Fig. 7B) and spanning amygdalae to thalami (Fig. 7C) are greater in the postoperative group. Differences specific to the cortical surface are located in the frontal region (Fig. 7A). First, the distances between the superior frontal sulci and their contralateral central sulci are greater in the postoperative group (Fig. 7A). Second, the distances between the frontal poles and the right superior frontal sulcus (Fig. 7A,E), and between the left frontal pole and the left inferior frontal sulcus (Fig. 7A,F) are increased in the postoperative sample.

Measures that are greater in the preoperative ISS sample as compared with the postoperative ISS group at Age B are oriented predominantly anteroposteriorly, both cortically and subcortically (Fig. 7, white lines). Many of these differences converge to the parietal region, particularly on the right side. Distances spanning from the right posterior lateral ventricle to the anterior lateral ventricles, the genu of the corpus callosum, the left caudate nucleus, the right thalamus, the frontal poles (Fig. 7B) and the inferior frontal sulci (Fig. 7C) are all increased in the preoperative group relative to the postoperative sample at Age B. The corresponding distances on the left side do not differ in postoperative as compared with older preoperative patients. Distances from the thalami to their ipsilateral caudate nuclei, anterior lateral ventricles and the genu of the corpus callosum are also increased in the preoperative group at this age (Fig. 7B). Finally, the distance between the inferior frontal sulcus and the Sylvian fissure is larger bilaterally in the preoperative group as compared with the postoperative group (Fig. 7A,E,F). The single mediolaterally oriented distance that is greater in the older preoperative group is the distance between the frontal poles (Fig. 7A).

These results indicate that surgery on the cranial vault is associated with an anteroposterior shortening of distances spanning the cortex and subcortex of the parietal region, but with an anteroposterior expansion of the frontal cortex. Cranial reconstructive surgery also appears to be associated with inferior displacement of the amygdalae in the anterior temporal poles.

## Discussion

Craniofacial development is a complex and highly integrated process, requiring the action of many genes and interactions at the molecular, cellular, tissue and gross

anatomical levels (e.g. Noden, 1983; LeDouarin et al. 1993; Hall & Miyake, 1995, 2000; Opperman, 2000; Francis-West et al. 2003; Richman & Lee, 2003). Few studies have investigated the interplay between established tissues over the course of development in craniosynostosis.

Hypotheses regarding factors responsible for changes in ISS skull shape have been proposed from analyses of the skull and these are primarily of a biomechanical nature. For example, it has been postulated that the skulls of children affected with isolated sagittal craniosynostosis may have attained these dysmorphic shapes in part through overrotation of the occiput during development (Marsh & Vannier, 1986; Kaiser, 1988; Richtsmeier et al. 1991; DeLeon et al. 2001). Overrotation might occur due to crowding of the brain and a subsequent posteriorly projected growth deformation, though this is clearly not the only mechanism by which such an overrotation could occur.

Results of this study show that the overall scaphocephalic skull shape is mirrored in the observed anteroposterior expansion of the brain in preoperative isolated sagittal synostosis. However, analysis of the ISS central nervous system (CNS) phenotype details a posteriorly directed expansion of the brain, observed in both forebrain and hindbrain structures, with no concomitant anterior expansion. This posterior expansion of the forebrain is reflected in skull morphology as occipital prominences, but the localized posterior expansion of hindbrain structures determined in this study cannot be detected from analysis of the skull.

Differences quantified between the brains of unoperated ISS patients and unaffected individuals are similar in pattern and magnitude in the two age groups considered. This finding has two important implications. First, this suggests that CNS dysmorphology is not exaggerated or 'worsened' by growth during the first 2 years of life. Second, it indicates that CNS dysmorphology associated with isolated sagittal synostosis that is maintained at Age B is present early in postnatal development, suggesting that the developmental processes responsible for CNS dysmorphology occur prenatally. This hypothesis can only be tested through the assessment of prenatal tissues in animal models.

It has been shown that neurocranial surgery for ISS produces a more normal skeletal configuration (Kreiborg & Pruzansky, 1981; Kaiser, 1988; Marsh et al. 1991; Posnick et al. 1993; DeLeon et al. 2001; Perlyn et al. 2001), returning the neurocranium to a more globular

shape. Postoperative morphology of the CNS in sagittal synostosis differs substantially from the preoperative morphology. Although the outer surface geometry of the brain conforms to the corrected neurocranial shape, internal structures reorganize themselves in ways that cannot be predicted by the change in skull shape. The overall effect on the brain is a change in spatial organization that differs substantially from both the unaffected and the preoperative conditions. Consequently, our results indicate some reciprocal relationships in the developing skull and brain, as well as some more autonomous developmental properties.

The CNS, meninges and skull influence each other's development during both pre- and postnatal periods. Studies of craniofacial development show that the CNS develops substantially earlier and more rapidly than cranial skeletal elements during the prenatal period, suggesting that neural tissue may provide a template around which the skull forms (reviewed in Burdi, 1976; Gasser, 1976; Kjaer, 1990; Lieberman et al. 2000; Redies & Puelles, 2001). There is some experimental evidence that the brain influences the form of the skull by way of direct physical and developmental connections with the physically intermediate dura (Moss, 1959; Moss & Young, 1960; Moss, 1977a,b,c,d; Enlow, 2000; Yu et al. 2001), leading to conclusions that growth of the brain places mechanical strain on sutural and non-sutural osteogenic cells through their connections with the dura.

Alternatively, experimental studies of grafted dural and skeletal tissues in normal and synostotic sutures suggest that dural tissue is independently responsible for suture patency, and therefore craniofacial morphology, via signalling mechanisms (Opperman et al. 1993, 1995, 1998; Bradley et al. 1996; Roth et al. 1996; Mooney et al. 2001). Recent studies have concluded that the trans-dural signals mediating suture fusion involve soluble factors, rather than biomechanical factors or cell-cell interactions (Opperman et al. 1993, 1995, 1998; Bradley et al. 1996; Roth et al. 1996; Mooney et al. 2001).

Whether the ultimate mechanism relating skull and brain morphology involves cell signalling mechanisms, biomechanical forces or a combination of these and other processes, it is clear that the growing CNS plays a significant role in the development of the skull (Hanken & Thorogood, 1993). However, its exact role remains unknown.

Following the tacit assumption that the fused suture is the primary cause of dysmorphology in craniosynostosis

(Marsh, 2000), the search for the definitive cause of craniosynostosis has focused on mutations in genes responsible for cranial bone formation, suture maintenance and suture closure (reviewed in Wilkie, 1997; Cohen & MacLean, 2000; DeLeon et al. 2000). Mutations have been identified in association with various forms of syndromic synostosis, but we remain largely uninformed about the relationship between gene action and the production of the craniosynostosis phenotype. No genetic mutation has yet been found in association with isolated sagittal synostosis.

We feel it prudent to consider that: (1) the fused suture is simply one link in the complex chain of events resulting in craniosynostosis phenotypes; (2) genetic mutations may not be the sole or the primary factor responsible for the non-syndromic craniosynostosis phenotype; (3) genetic pathways implicated in neural development, and not in bone formation, may be involved in certain craniosynostoses; and (4) the cause of non-syndromic craniosynostosis may be heterogeneous, with the closure of particular sutures more frequently associated with the nature of specific genetic backgrounds, the presence of given genetic anomalies or specific environmental conditions. By accepting these considerations, we adopt a line of thinking used in the study of the evolution of the mammalian skull, i.e. changes in the brain may be the basis for obvious changes in vertebrate skull phenotypes. The appearance of new skeletal phenotypes (changes in shape) and disappearance of cranial osseous elements over the course of evolution requires coordinated alterations in the developmental interplay between the skull and the brain. We suggest that the search for mutations responsible for craniosynostosis consider those genes and pathways that are important in formation of the brain.

In summary, the results of this study show that the morphology of the brain in craniosynostosis differs from normal both pre- and postoperatively, and that this dysmorphology includes both cortical and subcortical features. This indicates that the role of the development of the CNS should be reassessed with respect to the production of the most thoroughly studied craniosynostosis phenotype, that of the skull. The currently accepted developmental scenario assumes normal brain growth that is directly affected by a localized insult in skull growth dynamics. Our study suggests another scenario in which normal skull growth is outpaced by localized changing relationships in the brain. The meninges may also play a role as a mediator or even a

causative factor in the disproportionate growth of neural and skeletal craniofacial tissues. Whether the ultimate cause of craniosynostosis involves altered environmental conditions, the triggering of anomalous genetic cascades, cell signalling mechanisms, biomechanical forces or some combination of these factors, the CNS cannot be considered a passive tissue.

The fusion of the suture has been viewed as the point of origin in the production of the craniosynostosis phenotype, leading to the observed dysmorphogenesis associated with this condition. We may do better to consider fusion of the suture as a processional midpoint or even a phenotypic endpoint in a pathway of processes and interactions. Although much knowledge can be gained by studying each tissue type and the genes responsible for their development, the interplay of all tissues during development will eventually need to be considered. The craniofacial complex is a system that includes the skeleton, CNS, dura and other soft tissue organs and must be studied as a system. An understanding of the workings of this system will help us to begin to comprehend not only the etiologies associated with cranial developmental defects, but also the processes involved in the evolution of new cranial phenotypes.

## Acknowledgements

We thank Drs Mark Mooney, David Weishampel and Ralph Holloway for helpful comments on a previous version of this manuscript. This research has been supported in part by NIDCR grant 1 P60 DE13078.

## References

- Aldridge K, Barta P, Pearlson G, Richtsmeier J (2000) Brain morphology, MRI data, and landmark-based analyses of form. *Am. J. Phys. Anthropol. Suppl.* **30**, 94.
- Aldridge K, Marsh JL, Govier D, Richtsmeier JT (2002) Central nervous system phenotypes in craniosynostosis. *J. Anat.* **201**, 31–39.
- Aylward E, Augustine A, Li Q, Barta P, Pearlson G (1997) Measurement of frontal lobe volume on magnetic resonance imaging scans. *Psych. Res.* **75**, 23–30.
- Barritt J, Brooksbank M, Simpson D (1981) Scaphocephaly: aesthetic and psychosocial considerations. *Dev. Med. Child Neurol.* **23**, 183–191.
- Barta P, Dhingra L, Royall R, Schwartz E (1997) Improving stereological estimates for the volume of structures identified in three-dimensional arrays of spatial data. *J. Neurosci. Meth.* **75**, 111–118.
- Bradley JP, Levine JP, Blewett C, Krummel T, McCarthy JG, Longaker MT (1996) Studies in cranial suture biology: In vitro cranial suture fusion. *Cleft Palate Craniofac. J.* **33**, 150–156.
- Buchanan R, Vladar K, Barta P, Pearlson G (1998) Structural evaluation of the prefrontal cortex in schizophrenia. *Am. J. Psych.* **155**, 1049–1055.
- Burdi A (1976) Early development of the human basicranium: its morphogenic controls, growth patterns and relations. In *Symposium on Development of the Basicranium* (ed. Bosma J), pp. 81–90. Bethesda: U.S. Department of Health, Education, and Welfare.
- Carmel P, Luken M, Ascherl G (1981) Craniosynostosis: computed tomographic evaluation of skull base and calvarial deformities and associated intracranial changes. *Neurosurgery* **9**, 366–372.
- Cohen MM, MacLean RL (2000) *Craniosynostosis: Diagnosis, Evaluation, and Management*. New York: Oxford University Press.
- Cohen SR, Persing JA (1998) Intracranial pressure in single-suture craniosynostosis. *Cleft Palate Craniofac. J.* **35**, 194–196.
- Cooper G, Mooney M, Burrows A, et al. (1999) Brain growth rates in craniosynostotic rabbits. *Cleft Palate Craniofac. J.* **36**, 314–321.
- DeLeon VB, Jabs E, Richtsmeier JT (2000) Craniofacial growth: genetic basis and morphogenetic process in craniosynostosis. In *Craniofacial, Cleft, and Pediatric Surgery* (ed. Vander Kolk C), pp. 619–636. Philadelphia: Mosby.
- DeLeon VB, Zumpano MP, Richtsmeier JT (2001) The effect of neurocranial surgery on basicranial morphology in isolated sagittal craniosynostosis. *Cleft Palate Craniofac. J.* **38**, 134–146.
- Dufresne CR, McCarthy JG, Cutting CB, Epstein FJ, Hoffman WY (1987) Volumetric quantification of intracranial and ventricular volume following cranial vault remodeling: a preliminary report. *Plast. Reconstr. Surg.* **79**, 24–32.
- Enlow D (2000) Normal craniofacial growth. In *Craniosynostosis: Diagnosis, Evaluation, and Management* (eds Cohen MM, MacLean R), pp. 35–47. New York: Oxford University Press.
- Fok H, Jones B, Gault D, Andar U, Hayward R (1992) Relationship between intracranial pressure and intracranial volume in craniosynostosis. *Br. J. Plast. Surg.* **45**, 394–397.
- Francis-West PH, Robson L, Evans DJ (2003) Craniofacial development: the tissue and molecular interactions that control development of the head. *Adv. Anat. Embryol. Cell. Biol.* **169**, 1–138.
- Gasser R (1976) Early formation of the basicranium in man. In *Symposium on Development of the Basicranium* (ed. Bosma J), pp. 29–43. Bethesda: U.S. Department of Health, Education, and Welfare.
- Gault DT, Renier D, Marchac D, Ackland FM, Jones BM (1990) Intracranial volume in children with craniosynostosis. *J. Craniofac. Surg.* **1**, 1–3.
- Gault D, Renier D, Marchac D, Jones B (1992) Intracranial pressure and intracranial volume in children with craniosynostosis. *Plast. Reconstr. Surg.* **90**, 377–381.
- Hall BK, Miyake T (1995) Divide, accumulate, differentiate: cell condensations in skeletal development revisited. *Int. J. Dev. Biol.* **39**, 881–893.
- Hall BK, Miyake T (2000) All for one and one for all: condensations and the initiation of skeletal development. *Bioessays* **22**, 138–147.

- Hanken J, Thorogood P** (1993) Evolution and development of the vertebrate skull: the role of pattern formation. *TREE* **8**, 9–14.
- Kaiser G** (1988) Sagittal synostosis – its clinical significance and the results of three different methods of craniectomy. *Childs Nerv. Syst.* **4**, 223–230.
- Kjaer I** (1990) Ossification of the human fetal basicranium. *J. Craniofac. Genet. Dev. Biol.* **10**, 29–38.
- Kreiborg S, Pruzansky S** (1981) Craniofacial growth in premature craniofacial synostosis. *Scand. J. Plast. Reconstr. Surg.* **15**, 171–186.
- LeDouarin NM, Ziller C, Couly GF** (1993) Patterning of neural crest derivatives in the avian embryo: in vivo and in vitro studies. *Dev. Biol.* **159**, 24–49.
- Lele S** (1993) Euclidean Distance Matrix Analysis (EDMA): estimation of mean form and mean form difference. *Math. Geol.* **25**, 573–602.
- Lele S, Richtsmeier JT** (2001) *An Invariant Approach to the Statistical Analysis of Shapes*. London: Chapman & Hall-CRC Press.
- Lele S, McCulloch CE** (2002) Invariance, identifiability and morphometrics. *J. Am. Stat. Assoc.* **97**, 1–11.
- Lieberman D, Pearson O, Mowbray K** (2000) Basicranial influence on overall cranial shape. *J. Hum. Evol.* **38**, 291–315.
- Marsh JL, Vannier M** (1986) Cranial base changes following surgical treatment of craniosynostosis. *Cleft Palate Craniofac. J.* **23**, 9–18.
- Marsh JL, Jenny A, Galic M, Picker S, Vannier MW** (1991) Surgical management of sagittal synostosis. A quantitative evaluation of two techniques. *Neurosurg. Clin. North Am.* **2**, 629–640.
- Marsh JL, Lee B, Kane A, et al.** (1997) Brain tomographic dysmorphology in nonsyndromic craniosynostosis. In *Fifty-Fourth Annual Meeting of the American Cleft Palate-Craniofacial Association*. New Orleans (abstract).
- Marsh JL** (2000) Surgical research on craniosynostosis. In *Craniosynostosis: Diagnosis, Evaluation, and Management* (eds Cohen MM, MacLean RE), pp. 292–308. New York: Oxford University Press.
- Mooney M, Burrows A, Smith T, et al.** (2001) Correction of coronal suture synostosis using suture and dura mater allografts in rabbits with familial craniosynostosis. *Cleft Palate Craniofac. J.* **38**, 206–225.
- Moss ML** (1959) The pathogenesis of premature cranial synostosis in man. *Acta Anat.* **37**, 351–370.
- Moss ML, Young R** (1960) A functional approach to craniology. *Am. J. Phys. Anthropol.* **18**, 281–302.
- Moss ML** (1962) The functional matrix. In *Vistas in Orthodontics* (eds Kraus B Reidel R), pp. 85–98. Philadelphia: Lea & Febiger.
- Moss ML** (1997a) The functional matrix hypothesis revisited. 1. The role of mechanotransduction. *Am. J. Orthod. Dentofacial Orthop.* **112**, 8–11.
- Moss ML** (1997b) The functional matrix hypothesis revisited. 2. The role of an osseous connected cellular network. *Am. J. Orthod. Dentofacial Orthop.* **112**, 221–226.
- Moss ML** (1997c) The functional matrix hypothesis revisited. 3. The genomic Thesis. *Am. J. Orthod. Dentofacial Orthop.* **112**, 338–342.
- Moss ML** (1997d) The functional matrix hypothesis revisited. 4. The epigenetic antithesis and the resolving synthesis. *Am. J. Orthod. Dentofacial Orthop.* **112**, 410–417.
- Mouradian WE** (1998) Controversies in the diagnosis and management of craniosynostosis: a panel discussion. *Cleft Palate Craniofac. J.* **35**, 190–193.
- Noden DM** (1983) The role of the neural crest in patterning of avian cranial skeletal, connective, and muscle tissues. *Dev. Biol.* **96**, 144–165.
- Opperman L, Sweeney T, Redmon J, Persin J, Ogle R** (1993) Tissue interactions with underlying dura mater inhibit osseous obliteration of developing cranial sutures. *Dev. Dyn.* **98**, 312–322.
- Opperman L, Passarelli R, Morgan E, Reintjes M, Ogle R** (1995) Cranial sutures require tissue interactions with dura mater to resist osseous obliteration in vitro. *J. Bone Min. Res.* **10**, 1978–1987.
- Opperman L, Chhabra A, Nolen A, Bao Y, Ogle R** (1998) Dura mater maintains rat cranial sutures in vitro by regulating suture cell proliferation and collagen production. *J. Craniofac. Genet. Dev. Biol.* **18**, 150–158.
- Opperman LA** (2000) Cranial sutures as intramembranous bone growth sites. *Dev. Dyn.* **219**, 472–485.
- Perlyn CA, Marsh JL, Pilgram TK, Kane A** (2001) Plasticity of the endocranial base in nonsyndromic craniosynostosis. *Plast. Reconstr. Surg.* **108**, 294–301.
- Posnick JC, Bite U, Nakano P, Davis J, Armstrong D** (1992) Indirect intracranial volume measurements using CT scans: clinical applications for craniosynostosis. *Plast. Reconstr. Surg.* **89**, 34–45.
- Posnick JC, Lin KY, Chen P, Armstrong D** (1993) Sagittal synostosis: quantitative assessment of presenting deformity and surgical results based on CT scans. *Plast. Reconstr. Surg.* **92**, 1015–1024.
- Posnick J, Armstrong D, Bite U** (1995) Metopic and sagittal synostosis: intracranial volume measurements prior to and after cranio-orbital reshaping in childhood. *Plast. Reconstr. Surg.* **96**, 299–309.
- Redies C, Puelles L** (2001) Modularity in vertebrate brain development and evolution. *Bioessays* **23**, 1100–1111.
- Renier D, Lajeunie E, Arnaud E, Marchac D** (2000) Management of craniosynostoses. *Childs Nerv. Syst.* **16**, 645–658.
- Richman JM, Lee SH** (2003) About face: signals and genes controlling jaw patterning and identity in vertebrates. *Bioessays* **25**, 554–568.
- Richtsmeier JT, Grausz H, Morris G, Marsh J, Vannier M** (1991) Growth of the cranial base in craniosynostosis. *Cleft Palate Craniofac. J.* **28**, 55–67.
- Richtsmeier JT, Paik C, Elfert P, Cole T, Dahlman H** (1995) Precision, repeatability and validation of the localization of cranial landmarks using computed tomography scans. *Cleft Palate Craniofac. J.* **32**, 217–227.
- Roth DA, Bradley JP, Levine JP, McMullen HF, McCarthy JG, Longaker MT** (1996) Studies in cranial suture biology. 2. Role of the dura in cranial suture fusion. *Plast. Reconstr. Surg.* **97**, 693–699.
- Singhal VK, Mooney MP, Burrows AM, et al.** (1997) Age related changes in intracranial volume in rabbits with craniosynostosis. *Plast. Reconstr. Surg.* **100**, 1121–1128, 1129–1130.

**Valeri C, Cole T, Lele S, Richtsmeier J** (1998) Capturing data from three-dimensional surfaces using fuzzy landmarks. *Am. J. Phys. Anthropol.* **107**, 113–124.

**Virchow R** (1851) Über den Cretinismus, namentlich in Franken, und über pathologische Schädelformen. *Verh. Phys. Med. Gesellsch Würzburg.* **2**, 230–270.

**Wilkie AO** (1997) Craniosynostosis: genes and mechanisms. *Hum. Mol. Genet.* **6**, 1647–1656.

**Yu J, Lucas J, Fryberg K, Borke J** (2001) Extrinsic tension results in FGF-2 release, membrane permeability change, and intracellular Ca<sup>++</sup> increase in immature cranial sutures. *J. Craniofac. Surg.* **12**, 391–398.